Investigation of Dynamic Behavior of the Bray−Liebhafsky Reaction in the CSTR. Determination of Bifurcation Points

V. Vukojević,* S. Anić, and Lj. Kolar-Anić

Faculty of Physical Chemistry, University of Belgrade, P.O. Box 137, YU-11001 Belgrade, Yugoslavia

Received: March 28, 2000; In Final Form: July 19, 2000

Experimental results obtained by operating the Bray−Liebhafsky (BL) reaction in the CSTR are presented. The dynamic behavior of the BL reaction is examined at several operation points in the concentration phase space, by varying different parameters, the specific flow rate, temperature, and mixed inflow concentrations of the feed species, one at a time. Different types of bifurcation leading to simple periodic orbits, supercritical and subcritical Hopf bifurcations, saddle node infinite period bifurcation (SNIPER), saddle loop infinite period bifurcation, and jug handle bifurcation, are observed. Moreover, complex dynamic behavior, including transition from simple periodic oscillations to complex mixed-mode oscillations and chaos, and bistability are also discovered.

Introduction

The reaction of hydrogen peroxide decomposition, catalyzed by H^+ and IO_3^-

$$2H_2O_2 \xrightarrow{H^+,\ IO_3^-} O_2 + 2H_2O$$

is long known to exhibit nonlinear behavior. Since the first report of this reaction by Bray,[1] it was extensively investigated by Liebhafsky[2] and was after them named the Bray−Liebhafsky (BL) reaction. The pioneering work of Bray and Liebhafsky was carried on by many investigators, and considerable work is devoted to studying properties of the BL reaction and its mechanism, both in real experiments[3,4] and by theoretical analysis with corresponding numerical simulation.[2c,d,5] It is, however, remarkable that only a small fraction of this impressive body of work was conducted in the CSTR.[4] All remaining work, treats the BL reaction in the batch reactor.[1−3,5]

We rapport here the experimental results obtained by operating the BL reaction in the CSTR. In this paper we have examined, at several operation points, the dynamic behavior of the BL reaction by varying different parameters, the specific flow rate, temperature, and mixed inflow concentrations of the feed species, one at a time. We have found conditions where transition from a stationary state to periodic oscillations, and vice versa, undergoes through supercritical and subcritical Hopf bifurcation, the saddle node infinite period bifurcation (SNIPER), and the saddle loop infinite period bifurcation. Dynamic behavior, as a transition from simple periodic oscillations to complex mixed-mode oscillations and chaos, and bistability have been also discovered.

There are only few studies of the Bray−Liebhafsky reaction in the CSTR.[4] However, they are necessary for testing models of the BL reaction. They are also important for unraveling the chemistry of another oxy-halogen oscillator, the Briggs−Rauscher reaction,[6] as well as for different applications, for example, for analytical purposes with an aim to measure concentrations that are below current detection limits[7] or with an aim to depict kinetic characteristics of catalysts.[8]

Experimental Section

We have investigated a version of the BL reaction in which sulfuric acid is the source of H^+ and potassium iodate is the source of IO_3^-. Hydrogen peroxide, the true reactant that undergoes decomposition during the course of the BL reaction, is the remaining feed substance. Though the role of the mentioned feed substances in the overall reaction is obviously different, we sometimes, for simplicity, refer to all of them as reactants.

All reagents are commercial analytical grade and were used without any further purification. Deionized water of specific resistance $\rho = 18\ M\Omega\ cm^{-1}$ is used throughout.

The reaction was carried out in a continuously fed stirred tank reactor (CSTR). In all experiments, the feed substances, aqueous solutions of H_2SO_4, KIO_3, and H_2O_2, were kept in reservoirs at room temperature and were introduced into the reaction vessel separately and without being previously thermostated.

The volume of the reaction mixture was kept constant by suction through an U-tube, ending at the free surface over the reaction mixture. All flows, inflows of the reactants and outflow of the excess of reaction mixture, were generated by peristaltic pumps.

In all experiments, except **1a**, a reaction vessel, in the shape of an upside down frustum of a cone was used. The reaction vessel was made of glass, surrounded by a thermostat jacket, and was light protected, except in experiments **1c** and **3**. In the experiment described under **1a**, the reaction was conducted in a rectangular reaction vessel (2 cm × 5 cm × 6 cm) made of quartz, which was shielded from light.

The volume of the reaction mixture was always smaller than the volume of the reaction vessel, regardless of its shape. Therefore, a free surface over the reaction mixture allowed gas exchange between the phases. The gaseous phase over the reaction mixture was in contact with the atmosphere through a cylindrical hole on the lid (diameter 1 mm) and was flown out

* Corresponding author. E-mail: vladana@eunet.yu.

10.1021/jp001165x CCC: $19.00
Published on Web 10/21/2000

together with the excess of the reaction mixture. The rate, denoted as v_g, at which the gaseous phase is removed by the outflow was determined by measuring the volume of gas collected in a gas buret, in a unit of time. The rate at which the gaseous phase above the liquid reaction mixture is removed was also varied, since it is known that oxygen and iodine influence the overall reaction and, hence, its dynamics.[3c,5b−e]

The reaction mixture was stirred by a magnetic stirrer. The stirring rate, denoted as *o*, is different in different experiments, but the effect of stirring on the observed dynamic behavior was not investigated.

The temperature was maintained by a circulating water bath and controlled within ±0.2 °C.

Dynamics of the BL reaction was monitored potentiometrically. An Ag^+/S^{2-} ion-sensitive electrode (Metrohm, 6.0502.180), already defined as a sensor for iodine species,[3g,7,9] was used for monitoring the dynamics of the system. A double junction Ag/AgCl electrode (Metrohm, 6.0726.100) was used as a reference in all experiments except **1a**, where a saturated mercurous sulfate electrode (Radiometer K601) was used for the same purpose. In the reference Ag/AgCl electrode, the inner electrolyte was a 3.0 mol dm^{-3} solution of KCl and the outer electrolyte was a saturated solution of K_2SO_4. The potential output was recorded on a chart recorder and/or sampled, converted by a 12 bit ADC, and stored in the computer.

Distinctive properties of the experimental setup, as the start up procedure, the quantitative values of the volume of the reaction mixture, the rate at which the gaseous phase above the reaction mixture is removed, and the stirring rate, as well as deviations from the described setup, are indicated separately.

For all investigated operation points, the BL reaction was run at elevated temperatures. Working at elevated temperatures causes inevitable evaporation of the reaction mixture. This is an obstacle, especially when working at low values of the specific flow rate. Here the experiments have to be run continuously for several weeks. After such a long time, white crystal deposits collect at free surfaces, the lid and walls of the reaction vessel, the electrodes, and the suction U-tube bodies, which are not immersed in the reaction mixture. The composition of the crystals is not investigated. Repeatability of the experiments is checked by running the whole sequence in a different order. In general, no influence was observed, unless the crystals crumble and fall into the reaction mixture. In this case, the experiments have to be stopped and started anew.

Another impediment is the evaporation of the electrolytes from the reference electrode. This causes a change of the measured potential value. Therefore fresh electrolytes were added each morning in both the inner and the outer electrolytes compartment.

Results and Discussion

We have examined properties of the BL reaction, at different operation points in the concentration phase space. In addition, different parameters, the specific flow rate, temperature, and mixed inflow concentrations of the feed substances, were varied one at a time, and their influence on the dynamic behavior was investigated. All thus obtained results are summarized in Table 1.

1. Variation of the Specific Flow Rate. Dynamic behavior of the BL reaction is examined by variation of the flow rate at four different points in the concentration phase space. At all investigated points only transition from a stable nonequilibrium stationary state to simple periodic oscillations, and vice versa, is found. Four types of bifurcation from a stationary to an

TABLE 1: Experimental Conditions and Bifurcation Types Determined in the Bray−Liebhafsky Reaction

no.	$[H_2O_2]_0$/mol dm^{-3}	$[KIO_3]_0$/mol dm^{-3}	$[H_2SO_4]_0$/mol dm^{-3}	*T*/°C	j_0/min^{-1}	v_g/mL min^{-1}	*o*/rpm	crit value of bifurcatn param	bifurcatn type[b]
1a (Fig 1)	1.18×10^{-1}	6.59×10^{-2}	5.65×10^{-2}	46.5	$3.5 \times 10^{-3} - 4.75 \times 10^{-2}$	not measd	600	$j_0 = 2.90 \times 10^{-2}$ min^{-1}	supercrit Hopf
1b (Fig 2)	2.50×10^{-1}	6.10×10^{-2}	6.10×10^{-2}	60.0	$6.1 \times 10^{-3} - 3.61 \times 10^{-1}$	10.5	600	$j_0 = 1.295 \times 10^{-1}$ min^{-1}	SNIPER
1c[a] (Fig 3)	7.0×10^{-3}	7.50×10^{-2}	6.00×10^{-2}	60.0	$5.0 \times 10^{-4} - 6.33 \times 10^{-2}$	17.9	900	$j_0 = 1.05 \times 10^{-3}$ min^{-1}	Hopf
								$j_0 = 2.77 \times 10^{-2}$ min^{-1}	SNIPER
1d (Figs 4, 5)	1.55×10^{-1}	4.74×10^{-2}	4.79×10^{-2}	60.0	$8.1 \times 10^{-4} - 1.22 \times 10^{-1}$	17.9	900	$j_0 = 1.38 \times 10^{-3}$ min^{-1}	Subcrit Hopf[c]
								$j_0 = 4.94 \times 10^{-2}$ min^{-1}	Saddle loop[c]
2a (Fig 6)	2.00×10^{-1}	5.90×10^{-2}	5.50×10^{-2}	45.0− 57.5	2.96×10^{-2}	5.8	900	$T = 49.6$ °C	Supercrit Hopf
2b	2.50×10^{-1}	6.10×10^{-2}	6.10×10^{-2}	52.5− 61.5	1.10×10	5.8	1200	$T = 54.0$ °C	Supercrit Hopf
2c (Fig 7)	1.55×10^{-1}	4.74×10^{-2}	4.79×10^{-2}	45.0− 60.0	3.24×10^{-3}	17.9	900	$T = 47.6$ °C	sss to chaos
								$T = 52.8$ °C	chaos to simpleperiodic osc.
2d (Fig 8)	2.50×10^{-1}	5.58×10^{-2}	5.58×10^{-2}	54.0− 60.0	1.12×10^{-1}	17.9	900	$T = 57.3$ °C	sss to mixed-mode osc.
2e (Fig 9)	7.0×10^{-3}	7.50×10^{-2}	6.00×10^{-2}	35.0− 60.4	4.48×10^{-3}	17.9	900	$T = 39.2$ °C	jug handle
3[a] (Fig 10)	2.40×10^{-1}	3.46×10^{-2}	6.3×10^{-3} – 1.26×10^{-1}	60.0	3.82×10^{-2}	10.5	900	$[H_2SO_4]_0 = 5.56 \times 10^{-2}$	SNIPER
								$[H_2SO_4]_0 = 7.88 \times 10^{-2}$	mixed-mode osc to sss
4	2.40×10^{-1}	$6.3 \times 10^{-3} - 6.30 \times 10^{-2}$	6.31×10^{-2}	60.0	3.82×10^{-2}	10.5	900	$[KIO_3]_0 = 3.08 \times 10^{-2}$	SNIPER
5	$4.8 \times 10^{-2} - 2.40 \times 10^{-1}$	3.46×10^{-2}	6.31×10^{-2}	60.0	3.82×10^{-2}	10.5	900	$[H_2O_2]_0 = 2.37 \times 10^{-1}$	unidentified

[a] The reaction vessel was not shielded against light. [b] Locations of supercritical Hopf bifurcation points **1a**, **2a**, and **2b** are determined from the intercept on the abscissa of the linear extrapolation of the plot $A^2 = f$(bifurcation parameter). The values given for all other bifurcation types, correspond to the mean value of the bifurcation parameter obtained from the two adjacent experiments which are lying on both sides of the bifurcation point. [c] Hysteresis is observed for the both bifurcation types. Given values correspond to the critical values obtained when the specific flow rate is increased. In the reverse direction, the disappearance of the oscillations via a subcritical Hopf bifurcation appears at $j_0 = 8.9 \times 10^{-4}$ min^{-1}, if the initial point corresponds to 1.46×10^{-3} $min^{-1} \leq j_0 \leq 4.86 \times 10^{-3}$ min^{-1}. If the initial point corresponds to $j_0 > 4.86 \times 10^{-3}$ min^{-1}, the system remains on the upper stationary state branch for all investigated values of j_0.

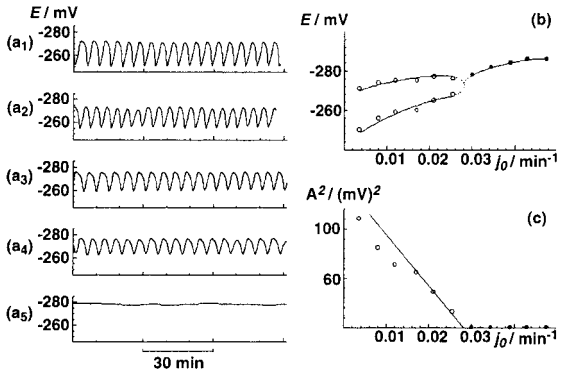

Figure 1. Time series observed in the BL reaction under conditions **1a**, when the specific flow rate, j_0, was varied from 3.5×10^{-3} to 4.75×10^{-2} min^{-1}: (a$_1$) $j_0 = 3.5 \times 10^{-3}$ min^{-1}; (a$_2$) $j_0 = 8.0 \times 10^{-3}$ min^{-1}; (a$_3$) $j_0 = 1.70 \times 10^{-2}$ min^{-1}; (a$_4$) $j_0 = 2.10 \times 10^{-2}$ min^{-1}; (a$_5$) $j_0 = 3.00 \times 10^{-2}$ min^{-1}. (b) A bifurcation diagram showing the envelope of the oscillations (circles) and the locus of the stable nonequilibrium stationary state (dots). (c) Plot of the square of the amplitude of the oscillations as a function of the specific flow rate j_0. The abscissa intercept corresponds to the bifurcation value of the specific flow rate, $j_0 = 2.90 \times 10^{-2}$ min^{-1}. The linearity of this plot in the vicinity of the bifurcation point, shows that the Hopf bifurcation is supercritical.

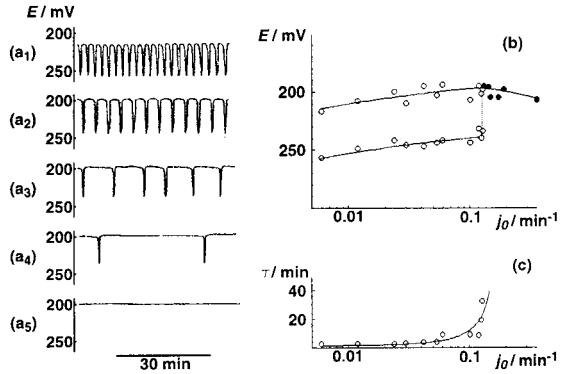

Figure 2. Time series observed in the BL reaction under conditions **1b**, when the specific flow rate, j_0, was varied from 6×10^{-3} to 3.61×10^{-1} min^{-1}: (a$_1$) $j_0 = 6 \times 10^{-3}$ min^{-1}; (a$_2$) $j_0 = 4.20 \times 10^{-2}$ min^{-1}; (a$_3$) $j_0 = 1.20 \times 10^{-1}$ min^{-1}; (a$_4$) $j_0 = 1.29 \times 10^{-1}$ min^{-1}; (a$_5$) $j_0 = 1.30 \times 10^{-1}$ min^{-1}. (b) A bifurcation diagram showing the envelope of the oscillations (circles) and the locus of the stable nonequilibrium stationary state (dots). The bifurcation occurs at $j_0 = 1.295 \times 10^{-1}$ min^{-1}. Hysteresis was not observed. (c) Plot of the period of the simple periodic oscillations as a function of the specific flow rate j_0.

oscillatory state are observed. Stationary state multiplicity, combined with a Hopf bifurcation, is also discovered.

a. The reaction was conducted in a rectangular reaction vessel (2 cm × 5 cm × 6 cm) made of quartz. Gaseous N_2 was bubbled through the reactant's solutions in the reservoirs and was blown above the free surface over the reaction mixture. The volume of the reaction mixture was kept constant at $V = (38.25 \pm 0.05)$ mL. The reaction mixture was stirred by a stirrer shaped as a triangular prism, driven by an electric motor, at a stirring rate $o = 600$ rpm. Only in this experiment, a saturated mercurous sulfate electrode was used as a reference.

The experiment commences by pipetting 20.0 mL of $[KIO_3] = 1.25 \times 10^{-1}$ mol dm^{-3} and 10.0 mL of $[H_2SO_4] = 2.40 \times 10^{-1}$ mol dm^{-3} from the reservoirs into the thermostated reaction vessel. The mixture of potassium iodate and sulfuric acid was thermostated about 30 min, and 10.0 mL of $[H_2O_2] = 5.00 \times 10^{-1}$ mol dm^{-3} was added. The reaction was run under batch conditions at temperature $T = 51.5$ °C, until the end of the last oscillation. Afterward, the flows were turned on and the specific flow rate was set to the highest investigated value, $j_0 = 4.75 \times 10^{-2}$ min^{-1}. (The gaseous phase removal rate was not measured.)

Under the conditions mixed inflow concentrations, $[KIO_3]_0 = 6.59 \times 10^{-2}$ mol dm^{-3}, $[H_2SO_4]_0 = 5.65 \times 10^{-2}$ mol dm^{-3}, $[H_2O_2]_0 = 1.18 \times 10^{-1}$ mol dm^{-3}, temperature $T = 46.5$ °C, and $o = 600$ rpm, the specific flow rate, j_0, was varied from 3.5×10^{-3} to 4.75×10^{-2} min^{-1}. In the interval 3.00×10^{-2} min$^{-1} \leq j_0 \leq 4.75 \times 10^{-2}$ min^{-1} stationary states are reached, whereas stable periodic oscillations exist for specific flow rate values from 3.5×10^{-3} to 2.55×10^{-2} min^{-1}. The observed dynamic behavior is presented in Figure 1a.

Transition from the stationary state into oscillatory goes through a supercritical Hopf bifurcation. The stationary state locus, together with the envelope of the oscillations, is given in Figure 1b. The bifurcation point, $j_0 = 2.90 \times 10^{-1}$ min^{-1}, is found by linear extrapolation of a plot of the square of the amplitude of the limit cycle oscillations versus the specific flow rate (Figure 1c).[10] [By definition, the amplitude is half the peak-to-peak difference for sinusoidal oscillations.]

b. The applied setup is as described in the Experimental Section. The start-up procedure was performed in the following way. First, the thermostated reaction vessel was filled up by the inflows of the reactants, at a maximal speed (7.5 mL min^{-1}). It was allowed that double of the reaction mixture volume (around 44 mL) flows into the vessel. Then the inflows were stopped, the stirrer was turned on, and the excess of the reaction mixture was sucked out through the U-shaped glass tube, to reach the actual reaction mixture volume, $V = (22.2 \pm 0.2)$ mL. The reaction commences under batch conditions. After three batch oscillations the inflows were turned on, and the temperature was adjusted to the working value. In this particular experiment, at the beginning the inflow was always adjusted to the highest value, $j_0 = 3.61 \times 10^{-1}$ min^{-1}.

Under the conditions $[KIO_3]_0 = 6.10 \times 10^{-2}$ mol dm^{-3}, $[H_2SO_4]_0 = 6.10 \times 10^{-2}$ mol dm^{-3}, $[H_2O_2]_0 = 2.50 \times 10^{-1}$ mol dm^{-3}, $T = 60.0$ °C, $o = 900$ rpm, and $v_g = 10.5$ mL min^{-1}, the specific flow rate was varied from 6.1×10^{-3} to 3.61×10^{-1} min^{-1}. Stationary states are found when the specific flow rate is in the range 1.30×10^{-1} min$^{-1} \leq j_0 \leq 3.61 \times 10^{-1}$ min^{-1}, whereas stable periodic oscillations exist for specific flow rate values 6.1×10^{-3} min$^{-1} \leq j_0 \leq 1.29 \times 10^{-1}$ min^{-1}. The observed dynamic behavior is presented in Figure 2a.

From the time series presented in Figure 2a, it is evident that the period of the oscillations increases whereas their amplitudes remain constant, when the bifurcation point is approached. The stationary state locus, together with the envelope of the oscillations, is given in Figure 2b. When the bifurcation point is approached, the period of the oscillations increases, and in the vicinity of the bifurcation point, oscillations with a period four times longer than the residence time endure. The observed exponential growth of the period of oscillations is presented in Figure 2c.

The bifurcation occurs at the same value of the specific flow rate, $j_0 = 1.29 \times 10^{-1}$ min^{-1}, when approached from either side; i.e., hysteresis was not observed.

The described properties are characteristic of the saddle node infinite period (SNIPER) bifurcation.[11]

c. At another operating point, $[KIO_3]_0 = 7.50 \times 10^{-2}$ mol dm^{-3}, $[H_2SO_4]_0 = 6.00 \times 10^{-2}$ mol dm^{-3}, $[H_2O_2]_0 = 7.0 \times 10^{-3}$ mol dm^{-3}, $T = 60.0$ °C, $o = 900$ rpm, and $v_g = 17.9$ mL min^{-1}, the specific flow rate, j_0, was varied from 5.0×10^{-4} to 6.33×10^{-2} min^{-1}. The same experimental setup and start-up procedure, as described in subsection **1b** were applied, except that the reaction vessel was not shielded against light.

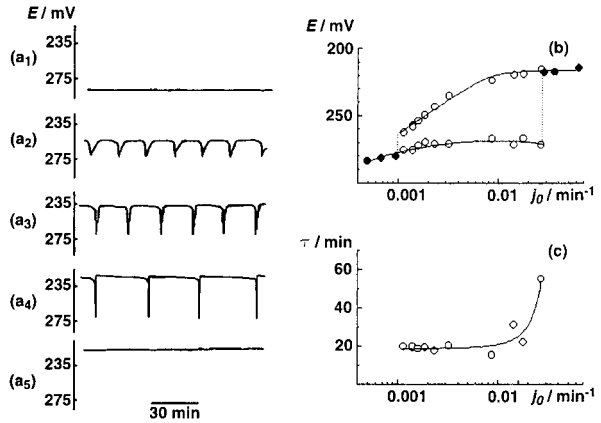

Figure 3. Time series observed in the BL reaction under conditions **1c**, when the specific flow rate, j_0, was varied from 5.0×10^{-4} to 6.33×10^{-2} min^{-1}: (a$_1$) $j_0 = 5.0 \times 10^{-4}$ min^{-1}; (a$_2$) $j_0 = 1.59 \times 10^{-3}$ min^{-1}; (a$_3$) $j_0 = 3.23 \times 10^{-3}$ min^{-1}; (a$_4$) $j_0 = 1.43 \times 10^{-2}$ min^{-1}; (a$_5$) $j_0 = 2.67 \times 10^{-1}$ min^{-1}. (b) A bifurcation diagram showing the envelope of the oscillations (circles) and the locus of the stable nonequilibrium stationary state (dots). The lower bifurcation occurs at $j_0 = 1.05 \times 10^{-3}$ min^{-1}, whereas the upper bifurcation occurs at $j_0 = 2.77 \times 10^{-2}$ min^{-1}. Hysteresis was not observed on either of the bifurcation points. (c) Plot of the period of the simple periodic oscillations as a function of the specific flow rate j_0.

Under these conditions, distinct stable nonequilibrium stationary states separated by an oscillatory evolution are found. The stationary states characterized by high potential values are found when the specific flow rate is in the range 5.0×0^{-4} min^{-1} $\leq j_0 \leq 9.6 \times 10^{-4}$ min^{-1}. Simple periodic oscillations exist for specific flow rate values in the interval 1.14×10^{-3} min^{-1} $\leq j_0 \leq 2.67 \times 10^{-2}$ min^{-1}, whereas stationary states characterized by low potential values are found when the specific flow rate is varied in the interval 2.87×10^{-2} min^{-1} $\leq j_0 \leq 6.33 \times 10^{-2}$ min^{-1}. The observed time series and corresponding bifurcation diagrams are given in Figure 3.

The lower bifurcation point occurs for a specific flow rate value, $j_0 = 1.05 \times 10^{-3}$ min^{-1}. When this bifurcation point is approached, the period of the oscillations remains constant, within experimental error, while the amplitude decreases. The oscillations, observed close to the bifurcation point, are of small amplitude but clearly asymmetric (Figure 3a$_2$). However, transient sinusoidal small amplitude limit cycle oscillations are observed when the system passes through the same bifurcation point from either side. Hysteresis is not observed.

Although sustained small amplitude harmonic oscillations were not observed, but only relaxation type oscillations were found in the asymptotic state, the observed transient small amplitude sinusoidal oscillations may indicate that there is a focus point in the phase plane. This suggests an appearance (and disappearance) of a periodic orbit via a Hopf bifurcation. However, on the basis of these experiments, it is not possible to distinguish between the two existing types, supercritical and subcritical, of the Hopf bifurcation. One possibility may be that the observed bifurcation point is a supercritical Hopf bifurcation, but sustained harmonic oscillations were not observed either because the parameter region within which the limit cycle grows to a finite size is narrow and cannot be resolved fine enough by the applied experimental setup or because of imperfections.[12] Imperfections may arise, for example, from the forcing of the system by the flows.[12c] Another possibility may be that the observed bifurcation point is a subcritical Hopf bifurcation, but the region of bistability between the stable steady state and the stable limit cycle was not observed, because the parameter region is too narrow to be observed experimentally.

The higher bifurcation point occurs for a specific flow rate value, $j_0 = 2.77 \times 10^{-2}$ min^{-1}. When this bifurcation point is approached, the amplitude of the oscillations remains constant, within experimental error, while the period increases exponentially. Hysteresis is not observed. The described properties are characteristic of the saddle node infinite period (SNIPER) bifurcation.

Thus, we assume that the underlying dynamic structure consists of a stationary state loosing stability at the lower bifurcation point probably through a Hopf bifurcation. As the bifurcation parameter is increased the limit cycle grows, until a new stable steady state appears right on the limit cycle via a saddle node infinite period (SNIPER) bifurcation.

d. At another operating point, $[KIO_3]_0 = 4.74 \times 10^{-2}$ mol dm^{-3}, $[H_2SO_4]_0 = 4.79 \times 10^{-2}$ mol dm^{-3}, $[H_2O_2]_0 = 1.55 \times 10^{-1}$ mol dm^{-3}, $T = 60.0$ °C, $o = 900$ rpm, and $\upsilon_g = 17.9$ mL min^{-1}, the specific flow rate was varied in the interval 8.1×10^{-4} min^{-1} $\leq j_0 \leq 1.22 \times 10^{-1}$ min^{-1}. The same experimental setup and start-up procedure, as described in subsection **1b**, were applied.

Under these conditions, two distinct stable stationary states and one oscillatory are found. Yet, the dynamic structure is entangled by hysteresis on both bifurcation points.

When the specific flow rate is varied from 8.1×10^{-4} to 1.30×10^{-3} min^{-1}, the stable stationary states characterized by higher potential values are attained. By increase of the specific flow rate, a bifurcation point is being passed through, at $j_0 = 1.38 \times 10^{-3}$ min^{-1}, and simple periodic oscillations exist in an interval 1.46×10^{-3} min^{-1} $\leq j_0 \leq 4.86 \times 10^{-3}$ min^{-1}.

When the specific flow rate is increased further, an abrupt stop of the oscillatory evolution is observed at $j_0 = 4.94 \times 10^{-2}$ min^{-1}, and a stationary state branch, characterized by lower potential values, is reached for specific flow rate values in the range 5.02×10^{-3} min^{-1} $\leq j_0 \leq 1.22 \times 10^{-1}$ min^{-1}. Being once on this stationary state branch, the system "stays" on it although the specific flow rate is decreased beyond both bifurcation points. Namely, the BL system remains on this branch for all investigated values of the specific flow rate, 8.1×10^{-4} min^{-1} $\leq j_0 \leq 1.30 \times 10^{-3}$ min^{-1}.

However, when the specific flow rate is decreased starting from any oscillatory state, $j_0 \leq 4.86 \times 10^{-3}$ min^{-1}, the simple periodic oscillations exist until $j_0 = 9.7 \times 10^{-4}$ min^{-1}. At $j_0 = 8.1 \times 10^{-4}$ min^{-1} the initial stationary states branch is reached again. In a comparison of these results with the ones obtained when j_0 is increased, the hysteresis is noted.

Time series, showing the observed dynamic behavior, are presented in Figure 4. As can be seen from Figure 4, at the specific flow rate $j_0 = 1.30 \times 10^{-3}$ min^{-1}, at least three different experimentally determined dynamic states can be achieved. One oscillatory and two nonoscillatory ones but at different potentials.

The stationary states loci, together with the envelope of the oscillations, are given in Figure 5a. Figure 5b presents the period of the simple periodic oscillations versus the specific flow rate.

We deduce that the lower bifurcation point, appearing at $j_0 = 1.38 \times 10^{-3}$ min^{-1}, has characteristics of a subcritical Hopf bifurcation point. Whereas, the higher bifurcation point, occurring at $j_0 = 4.94 \times 10^{-2}$ min^{-1}, has characteristics of a saddle loop bifurcation point.[11] Here, we should note that it appears as if the growing limit cycle (denoted by circles in Figure 5a) touches the branch of the steady stable state characterized by

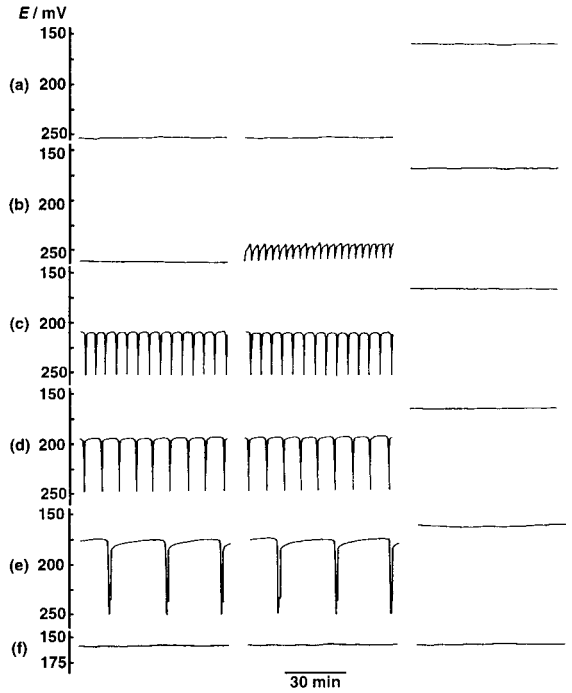

Figure 4. Time series observed in the BL reaction under conditions **1d**, when the specific flow rate, j_0, was varied from 8.1×10^{-4} to 1.22×10^{-1} min^{-1}: (a) $j_0 = 8.1 \times 10^{-4}$ min^{-1}; (b) $j_0 = 1.30 \times 10^{-3}$ min^{-1}; (c) $j_0 = 1.92 \times 10^{-3}$ min^{-1}; (d) $j_0 = 2.43 \times 10^{-3}$ min^{-1}; (e) $j_0 = 8.10 \times 10^{-3}$ min^{-1}; (f) $j_0 = 8.10 \times 10^{-3}$ min^{-1}. Time series given in the first column are attained when the specific flow rate is increased from an initial value $j_0 \leq 8.1 \times 10^{-4}$ min^{-1}. Time series given in the second column are attained when the initial value of the specific flow rate is 1.46×10^{-3} min^{-1} $\leq j_0 \leq 4.86 \times 10^{-3}$ min^{-1}. Time series given in the third column are attained when the initial value of the specific flow rate is $j_0 \geq 4.86 \times 10^{-3}$ min^{-1}.

the lower potential values (denoted by dots in Figure 5a) in the bifurcation point. Actually, this is not the case. As the bifurcation parameter is increased, the limit cycle grows. In the bifurcation point, it touches a saddle point and forms a homoclinic orbit. The oscillations terminate in the homoclinic orbit, and the systems ends at the stationary state characterized by the lower potential values. The basins of these two attractors are separated. However, the branch of the saddle point separating them cannot be seen as only attractors are observed in the experiments.

Thus, the simplest possible explanation for the observed multiplicity is that it may derive from a combination of stationary state multiplicity and a Hopf bifurcation. A subcritical Hopf bifurcation probably emerges along the lower shore of an isola. The limit cycle, growing from the subcritical Hopf bifurcation, terminates in a homoclinic orbit, and the system ends on the upper stationary state branch, characterized by low potential values. Once on this branch, it remains there for all investigated values of the specific flow rate.

2. Variation of the Temperature. The dynamic behavior of the BL reaction is examined at five different operation points in the concentration phase space. At each operation point the temperature is varied in a broad interval. Transitions from a stationary state to simple periodic oscillations through a supercritical Hopf bifurcation, the sequence of mixed-mode oscillations and the mixed mode chaos, are found.

a. A supercritical Hopf bifurcation is also found under the following conditions: $[KIO_3]_0 = 5.90 \times 10^{-2}$ mol dm^{-3}; $[H_2SO_4]_0 = 5.50 \times 10^{-2}$ mol dm^{-3}; $[H_2O_2]_0 = 2.00 \times 10^{-1}$ mol dm^{-3}; $j_0 = 2.96 \times 10^{-2}$ min^{-1}; $o = 900$ rpm; $v_g = 5.8$ mL min^{-1}. The temperature was varied from 45.0 °C $\leq T \leq$ 57.5 °C. The same experimental setup and start-up procedure, as described in subsection **1b**, were applied, the only differences being the volume of the reaction mixture ($V = (24.0 \pm 0.2)$ mL) and the inflows of the reactants at a maximal speed (16.0 mL min^{-1}).

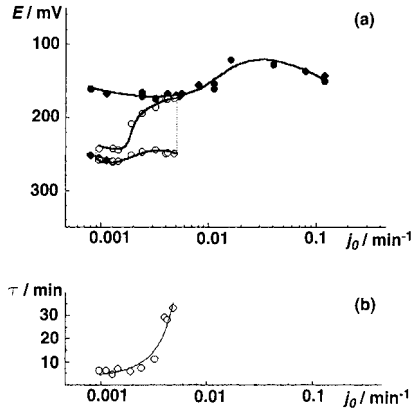

Figure 5. (a) A bifurcation diagram showing the envelope of the oscillations (circles) and the locus of the stable nonequilibrium stationary state (dots), for time series given in Figure 4. When one starts from the lowest investigated value of the specific flow rate, $j_0 = 8.1 \times 10^{-4}$ min^{-1}, the lower bifurcation occurs at $j_0 = 1.38 \times 10^{-3}$ min^{-1}, whereas the upper bifurcation occurs at $j_0 = 4.94 \times 10^{-2}$ min^{-1}. In this case, a dynamic change from a stable stationary state to an oscillatory one is observed at the lower bifurcation point, whereas the oscillations "die" out at the higher bifurcation point. Hysteresis was observed on both bifurcation points. Hence, when the bifurcation parameter is decreased, rather than increased, the oscillatory evolution that has emerged at the lower bifurcation point, $j_0 = 1.38 \times 10^{-3}$ min^{-1}, will endure until $j_0 = 8.9 \times 10^{-4}$ min^{-1}, when the bifurcation parameter is decreased, providing that the upper bifurcation point, occurring at $j_0 = 4.94 \times 10^{-2}$ min^{-1}, was not surpassed. When the upper bifurcation point is surpassed and the stationary state branch characterized by lower potential values is reached, the system remains on this branch even though the specific flow rate is changed backward down to the lowest investigated value, $j_0 = 8.1 \times 10^{-4}$ min^{-1}. (b) Plot of the period of the simple periodic oscillations as a function of the specific flow rate j_0.

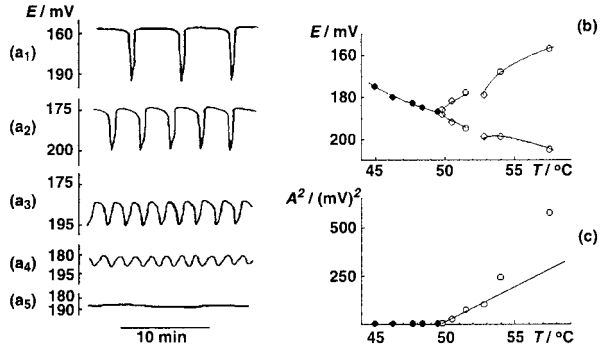

Figure 6. Time series observed in the BL reaction under conditions **2a**, when the temperature was varied from 45.0 to 57.5 °C: (a_1) $T =$ 57.5 °C; (a_2) $T = 52.8$ °C; (a_3) $T = 51.5$ °C; (a_4) $T = 50.5$ °C; (a_5) $T = 48.5$ °C. (b) A bifurcation diagram showing the envelope of the oscillations (circles) and the locus of the stable nonequilibrium stationary state (dots). (c) Plot of the square of the amplitude of the oscillations as a function of the temperature T. The abscissa intercept corresponds to the bifurcation value of the temperature, $T = 49.6$ °C. The linearity of this plot shows that the Hopf bifurcation is supercritical.

The time series are given in Figure 6a, and the stationary state locus, together with the envelope of the oscillations, is given in Figure 6b. The bifurcation point is found at $T = 49.6$ °C, by linear extrapolation of a plot of the square of the amplitude of the limit cycle oscillations versus temperature (Figure 6c).

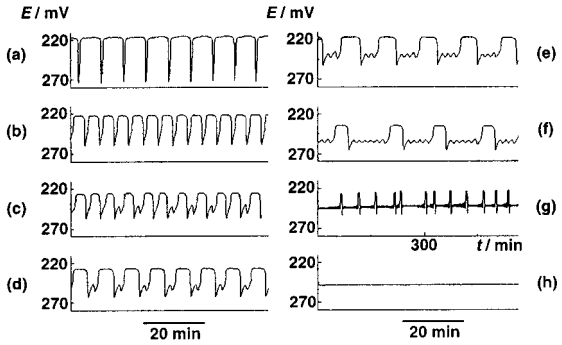

Figure 7. Time series observed in the BL reaction under conditions **2c**, when the temperature was varied from 45.0 to 60.0 °C: (a) T = 60.0 °C, large amplitude relaxation oscillations, 1^0; (b) T = 52.8 °C, 1^0; (c) T = 50.3 °C, chaos; (d) T = 49.8 °C, mixed-mode oscillations, 1^1; (e) T = 49.3 °C, chaos; (f) T = 48.8 °C, chaos; (g) T = 47.8 °C, chaos; (h) T = 47.6 °C, stable nonequilibrium stationary state.

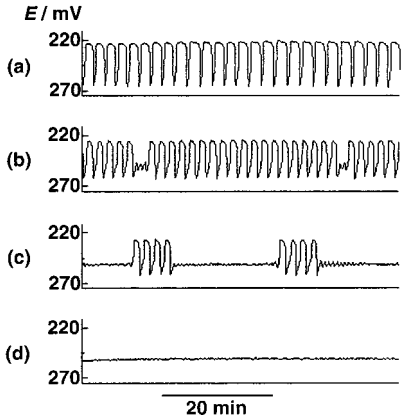

Figure 8. Time series observed in the BL reaction under conditions **2d**, when the temperature was varied from 54.0 to 60.0 °C: (a) T = 60.0 °C; (b) T = 58.0 °C; (c) T = 57.3 °C; (d) T = 56.4 °C.

In the temperature interval 49.8 °C $\leq T \leq$ 51.5 °C, the amplitude of the oscillations increases with the square root of the distance from the bifurcation point (Figure 6c), in accordance with the Hopf theorem.[10] This is no longer so when the temperature is increased further on. Namely, when $T >$ 51.5 °C, the amplitude of the oscillations grows abruptly, which may be due to a strong nonlinearity of the system in this parameter region. This may be associated with the change of the reaction pathway, which is known to occur in the BL reaction at temperatures around T = 52.0 °C.[3i,j]

b. Dynamic behavior of the BL reaction was investigated under the following conditions: $[KIO_3]_0 = 6.10 \times 10^{-2}$ mol dm^{-3}; $[H_2SO_4]_0 = 6.10 \times 10^{-2}$ mol dm^{-3}; $[H_2O_2]_0 = 2.50 \times 10^{-1}$ mol dm^{-3}; $j_0 = 1.10 \times 10^{-1}$ min^{-1}; o = 1200 rpm; v_g = 5.8 mL min^{-1}. The temperature was varied from 52.5 °C $\leq T \leq$ 61.5 °C. The same experimental setup and start-up procedure as described in subsection **1b** were applied.

The observed time series and the dynamics are of the same type as the ones presented in Figure 6. The transition from the stable stationary state into an oscillatory goes through a supercritical Hopf bifurcation. The bifurcation point, T = 54.0 °C, is found by linear extrapolation of a plot of the square of the amplitude of the limit cycle oscillations versus temperature.

c. Under the conditions $[KIO_3]_0 = 4.74 \times 10^{-2}$ mol dm^{-3}, $[H_2SO_4]_0 = 4.79 \times 10^{-2}$ mol dm^{-3}, $[H_2O_2]_0 = 1.55 \times 10^{-1}$ mol dm^{-3}, $j_0 = 3.24 \times 10^{-3}$ min^{-1}, o = 900 rpm, and v_g = 17.9 mL min^{-1}, the temperature was varied from 45.0 °C $\leq T \leq$ 60.0 °C. The same experimental setup and start-up procedure as described in subsection **1b** were applied.

For temperature values 52.8 °C $\leq T \leq$ 60.0 °C, simple periodic oscillations are found (Figure 7a,b). When the temperature is decreased below 52.8 °C, indications of the period doubling route to chaos are observed (Figure 7b,c).

Further down, in the temperature interval 48.8 °C $\leq T \leq$ 49.8 °C, periodic 1^1 mixed-mode oscillations and aperiodic mixed mode oscillations, with different mixing of the large and small oscillations,[11f] are detected (Figure 7d−f). [We adopt the L^s notation, where L and s are the number of large (L) and small (s) peaks per repeating unit.[11f]]

At the temperature T = 47.8 °C apparent intermittent behavior can be noticed (Figure 7g), and finally, for temperature values 45.0 °C $\leq T \leq$ 47.6 °C the system is found on a stable stationary state branch (Figure 7h).

At the temperature T = 47.7 °C, either small amplitude 0^1 oscillations or small amplitude chaos is observed. At present, we are unable to distinguish between the two. Namely, such behavior is found between a stationary state at T = 47.6 °C and a chaotic dynamic at T = 47.8 °C. Thus, the temperature interval is equal to the achieved temperature control (±0.2 °C). Therefore, a more rigorous temperature control has to be applied, to distinguish between the two possibilities.

d. At the same setup and start-up procedures as in subsection **1b** and the conditions $[KIO_3]_0 = 5.58 \times 10^{-2}$ mol dm^{-3}, $[H_2SO_4]_0 = 5.58 \times 10^{-2}$ mol dm^{-3}, $[H_2O_2]_0 = 2.50 \times 10^{-1}$ mol dm^{-3}, $j_0 = 1.12 \times 10^{-1}$ min^{-1}, o = 900 rpm, and v_g = 17.9 mL min^{-1}, the temperature was varied from 54.0 to 60.0 °C. Here, the stationary state branch loses stability when the temperature is increased over T = 56.4 °C, and mixed mode, burstlike, oscillations emerge. The number of large amplitude oscillations increases for increasing temperature, and for temperatures higher than T = 58.0 °C, simple periodic oscillations appear. The observed time series are given in Figure 8.

e. The experiment commences by pipetting 15.0 mL of $[KIO_3] = 1.50 \times 10^{-1}$ mol dm^{-3} and 7.5 mL of $[H_2SO_4] = 2.40 \times 10^{-1}$ mol dm^{-3} from the reservoirs into the thermostated reaction vessel. The mixture of potassium iodate and sulfuric acid was thermostated about 50 min, and 7.5 mL of $[H_2O_2] = 2.80 \times 10^{-2}$ mol dm^{-3} is added. The reaction was run under batch conditions at temperature T = 60.0 °C, until the end of the last batch oscillation. Afterward the flows were turned on, and the specific flow rate was set to the investigated value, $j_0 = 4.48 \times 10^{-3}$ min^{-1}. The volume of the reaction mixture was kept constant at V = (24.0 ± 0.2) mL. The experimental setup is described in the Experimental Section.

Under the conditions $[KIO_3]_0 = 7.50 \times 10^{-2}$ mol dm^{-3}, $[H_2SO_4]_0 = 6.00 \times 10^{-2}$ mol dm^{-3}, $[H_2O_2]_0 = 7.00 \times 10^{-3}$ mol dm^{-3}, $j_0 = 4.48 \times 10^{-3}$ min^{-1}, o = 900 rpm, and v_g = 17.9 mL min^{-1}, the temperature was varied from 35.0 °C $\leq T \leq$ 60.4 °C. For temperature values from 35.0 °C $\leq T \leq$ 38.7 °C stationary dynamic behavior is found, which changes to simple periodic oscillations when the temperature is $T \geq$ 39.8 °C. Simple periodic oscillations are observed in the whole investigated temperature interval, 39.8 °C $\leq T \leq$ 60.4 °C. The observed time series are given in Figure 9a.

When the bifurcation point is approached from the oscillatory side, the amplitude of the oscillations decreases, although in the two last experiments they were constant, whereas the period increases (Figure 9b,c). Hysteresis is not observed.

A possible theoretical explanation for the observed dynamic behavior may be that the oscillating behavior appears (and disappears) via a subcritical Hopf bifurcation connected with a jug handle bifurcation.[13] Namely, while the amplitude of the

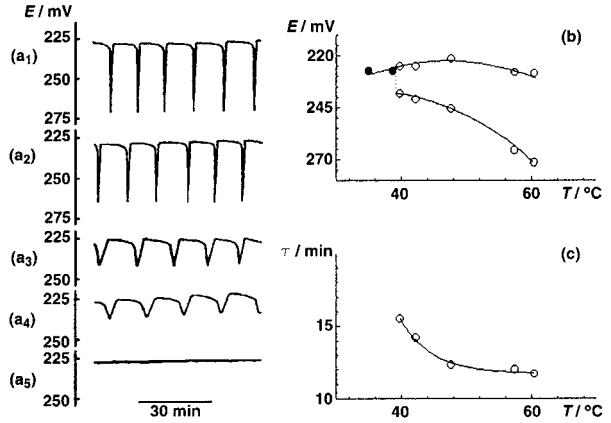

Figure 9. Time series observed in the BL reaction under conditions **2e**, when the temperature was varied from 35.0 to 60.4 °C: (a_1) T = 60.4 °C; (a_2) T = 46.1 °C; (a_3) T = 42.2 °C; (a_4) T = 39.8 °C; (a_5) T = 35.0 °C. (b) A bifurcation diagram showing the envelope of the oscillations (circles) and the locus of the stable nonequilibrium stationary state (dots). The bifurcation occurs at T = 39.2 °C. Hysteresis was not observed. (c) Plot of the period of the simple periodic oscillations as a function of the temperature T.

oscillations decreases considerably when approaching the bifurcation point, the increase of the time period is much less dramatic (Figure 9b,c). The observed small increase in the time period may indicate a nearby coalescence of the stable and unstable limit cycles,[13] and this can be connected with a subcritical Hopf bifurcation. As already discussed in section **1c**, the parameter region in which bistability occurs may be to narrow to observe experimentally the hysteresis.

We note that here the observed small amplitude oscillations are characterized by lower potential values. Whereas, in our experience with the BL reaction, the appearance of small amplitude oscillations is more often characterized by higher potential values.[3h,p,14]

3. Variation of the Mixed Inflow Concentration of Sulfuric Acid. To investigate the influence of the mixed inflow concentration of sulfuric acid, $[H_2SO_4]_0$, on the dynamic of the BL reaction, a setup described in the Experimental Section is applied, the only difference being that the reaction vessel was not shielded against light.

At the beginning of each experiment, the thermostated reaction vessel was first filled up by the inflows of the reactants at a maximal speed (16.0 mL min^{-1}). It was allowed that double of the reaction mixture volume (around 54 mL) flows into the vessel. Then the inflows were stopped, the stirrer was turned on, and the excess of the reaction mixture was sucked out, to reach the actual reaction mixture volume, V = (26.7 ± 0.2) mL. Then the inflows were turned on, the specific flow rate was set to the working value, $j_0 = 3.82 \times 10^{-2}$ min^{-1}, and the temperature was adjusted to the working value T = 60.0 °C.

Under the conditions $[KIO_3]_0 = 3.46 \times 10^{-2}$ mol dm^{-3}, $[H_2O_2]_0 = 2.40 \times 10^{-1}$ mol dm^{-3}, T = 60.0 °C, $j_0 = 3.82 \times 10^{-2}$ min^{-1}, o = 900 rpm, and v_g = 10.5 mL min^{-1}, the mixed inflow concentration of sulfuric acid was varied in a broad interval, 6.3×10^{-3} mol dm^{-3} ≤ $[H_2SO_4]_0$ ≤ 1.26×10^{-1} mol dm^{-3}.

The observed dynamic behavior is summarized in Table 2. As can be seen from Table 2, the stationary state branch characterized by lower potential values is followed by simple periodic oscillations of large amplitude. By an increase of the mixed inflow concentration of sulfuric acid, a region of mixed-mode oscillations is entered. The number of the large amplitude

TABLE 2: Dynamic Behavior Observed in the BL Reaction When the Mixed Inflow Concentration of Sulfuric Acid, $[H_2SO_4]_0$, Is Varied

$[H_2SO_4]_0$/mol dm^{-3}	dynamic behavior[a]	E_{max}/mV	E_{min}/mV	τ/min[b]
6.3×10^{-3}	sss	50	50	
1.58×10^{-2}	sss	74	74	
2.53×10^{-2}	sss	86	86	
3.47×10^{-2}	sss	93	93	
4.42×10^{-2}	sss	102	102	
4.96×10^{-2}	sss	105	105	
5.53×10^{-2}	sss	110	110	
5.60×10^{-2}	1^0	209	123	23.8
6.71×10^{-2}	1^0	211	137	11.0
7.20×10^{-2}	1^0	217	164	3.9
7.44×10^{-2}	1^0	216	172	2.1
7.53×10^{-2}	1^0	218	169	2.3
7.62×10^{-2}	6^{many}	219[c]	180[c]	19.4
7.72×10^{-2}	3^{many}	218[c]	180[c]	19.7
7.76×10^{-2}	chaos	216[c]	180[c]	
7.80×10^{-2}	1^{many}	215[c]	176[c]	19.5
7.96×10^{-2}	sss	202	202	
8.34×10^{-2}	sss	204	204	
9.00×10^{-2}	sss	212	212	
1.25×10^{-1}	sss	220	220	

[a] Dynamic behavior, denoted as sss, corresponds to a stable nonequilibrium stationary state. The L^s notation is adopted to denote the mixed-mode oscillations. [b] τ denotes the period of the oscillations. [c] Extreme potential values of the large amplitude oscillations are given.

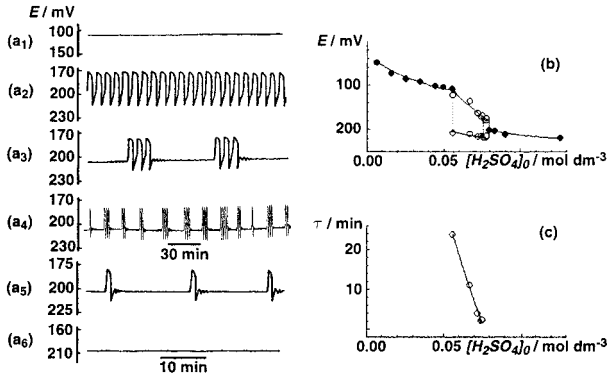

Figure 10. Time series observed in the BL reaction under conditions **3**, when the mixed inflow concentration of sulfuric acid, $[H_2SO_4]_0$, was varied from 6.3×10^{-3} to 1.25×10^{-1} min^{-1}: (a_1) $[H_2SO_4]_0 = 5.53 \times 10^{-2}$ mol dm^{-3}; (a_2) $[H_2SO_4]_0 = 7.44 \times 10^{-2}$ mol dm^{-3}; (a_3) $[H_2SO_4]_0 = 7.72 \times 10^{-2}$ mol dm^{-3}; (a_4) $[H_2SO_4]_0 = 7.76 \times 10^{-2}$ mol dm^{-3}; (a_5) $[H_2SO_4]_0 = 7.80 \times 10^{-2}$ mol dm^{-3}; (a_6) $[H_2SO_4]_0 = 7.96 \times 10^{-2}$ mol dm^{-3}. The 30 min time scale applies to the time series given in (a_4), only. The 10 min time scale applies in all other cases. (b) A bifurcation diagram showing the envelope of the oscillations (circles) and the locus of the stable nonequilibrium stationary state (dots). The lower bifurcation occurs at $[H_2SO_4]_0 = 5.56 \times 10^{-2}$ mol dm^{-3}, whereas the upper bifurcation occurs at $[H_2SO_4]_0 = 7.88 \times 10^{-2}$ mol dm^{-3}. Hysteresis was not observed on either of the bifurcation points. (c) Plot of the period of the simple periodic oscillations as a function of the mixed inflow concentration of sulfuric acid, $[H_2SO_4]_0$.

oscillations in the mixed-mode waveform decreases when the bifurcation parameter is increased. Between the periodic 3^{many} and 1^{many} waveforms, shown in Figure 10$a_{3,}a_{5,}$ respectively, an aperiodic dynamic, shown in Figure 10a_4, is observed. Eventually, a stationary state branch characterized by high potential values is reached.

The stationary state loci, together with the envelope of the oscillations, are given in Figure 10b. Figure 10c presents the period of the simple periodic oscillations, versus the mixed inflow concentration of sulfuric acid, $[H_2SO_4]_0$. Hysteresis is not observed either on one or the other bifurcation point.

Thus, the simplest possible explanation of the underlying dynamic structure exhibiting such dynamic behavior corresponds to a stationary state, characterized by law potential values, losing stability at the lower bifurcation point, via a SNIPER bifurcation. At the same point a homoclinic orbit is formed and sheds a stable limit cycle. The limit cycle oscillations undergo a transition to mixed-mode oscillations, and then an aperiodic window occurs, reverting again to the mixed-mode dynamics. At the higher bifurcation point, where the unstable stationary state regains its stability, the dynamics changes further on along the high potential stable nonequilibrium stationary state branch.

4. Variation of the Mixed Inflow Concentration of Potassium Iodate. The dynamic behavior of the BL reaction is investigated at the operation point in the concentration phase space $[H_2SO_4]_0 = 6.31 \times 10^{-2}$ mol dm^{-3}, $[H_2O_2]_0 = 2.40 \times 10^{-1}$ mol dm^{-3}, $T = 60.0$ °C, $j_0 = 3.82 \times 10^{-2}$ min^{-1}, $o = 900$ rpm, and $\upsilon_g = 10.5$ mL min^{-1}, by varying the mixed inflow concentration of potassium iodate, $[KIO_3]_0$, from 6.3×10^{-3} to 6.30×10^{-2} mol dm^{-3}. The experimental setup is described in section 3.

At this operation point, stationary states are observed when 6.3×10^{-3} mol dm$^{-3} \leq [KIO_3]_0 \leq 3.06 \times 10^{-2}$ mol dm^{-3}, and simple periodic oscillations are observed for mixed inflow concentrations 3.10×10^{-2} mol dm$^{-3} \leq [KIO_3]_0 \leq 6.30 \times 10^{-2}$ mol dm^{-3}. The amplitude of the oscillations is constant, within experimental error, while the period of the oscillations grows exponentially when the bifurcation point is approached. Hysteresis is not observed. Such behavior is typical for a SNIPER bifurcation.

5. Variation of the Mixed Inflow Concentration of Hydrogen Peroxide. The dynamic behavior of the BL reaction is investigated at the operation point in the concentration phase space $[KIO_3]_0 = 3.46 \times 10^{-2}$ mol dm^{-3}, $[H_2SO_4]_0 = 6.31 \times 10^{-2}$ mol dm^{-3}, $T = 60.0$ °C, $j_0 = 3.82 \times 10^{-2}$ min^{-1}, $o = 900$ rpm, and $\upsilon_g = 10.5$ mL min^{-1}, by varying the mixed inflow concentration of hydrogen peroxide, $[H_2O_2]_0$, from 4.80×10^{-2} to 2.40×10^{-1} mol dm^{-3}. The experimental setup is described in section 3.

At this operation point, stationary states are observed when the mixed inflow concentration of hydrogen peroxide is varied in the range 4.80×10^{-2} mol dm$^{-3} \leq [H_2O_2]_0 \leq 2.34 \times 10^{-1}$ mol dm^{-3}. When the $[H_2O_2]_0$ is further increased, to $[H_2O_2]_0 = 2.40 \times 10^{-1}$ mol dm^{-3}, large amplitude relaxation oscillations emerge. However, under these conditions a new phase, i.e. metal iodine, is formed. Further investigation was not carried out, because of the appearance of a new phase.

Conclusions

An elaborate investigation of the dynamic behavior exhibited by the BL reaction under different experimental conditions in the CSTR is performed. The reaction dynamics is investigated at 12 operation points in the concentration phase space. Different parameters, the specific flow rate, temperature, and mixed inflow concentrations of sulfuric acid ($[H_2SO_4]_0$), potassium iodate ($[KIO_3]_0$), and hydrogen peroxide ($[H_2O_2]_0$), were varied one at a time, at different operation points in the phase space. A total of 15 bifurcation points of different types were determined. Experimental evidence for the onset and termination of oscillatory behavior via the supercritical Hopf bifurcation and the saddle node infinite period (SNIPER) bifurcation are presented. Along with indications of changes in the dynamic behavior of the BL reaction occurring through a subcritical Hopf bifurcation, the saddle loop infinite period bifurcation and the jug handle bifurcation were noticed. Complex dynamic behavior, including transition from simple periodic oscillations to complex mixed-mode oscillations and chaos, and multistability were also discovered.

Acknowledgment. The authors thank an unknown reviewer for helpful suggestions regarding the theoretical description of some experimental observations.

References and Notes

(1) Bray, W. C. *J. Am. Chem. Soc.* **1921**, *43*, 1262.

(2) Bray, W. C.; Liebhafsky, H. A. *J. Am. Chem. Soc.* **1931**, *53*, 38. (b) Matsuzaki, I.; Woodson, J. H.; Liebhafsky, H. A. *Bull. Chem. Soc. Jpn.* **1970**, *43*, 3317. (c) Liebhafsky, H. A.; Wu, L. S. *J. Am. Chem. Soc.* **1974**, *96*, 7180. (d) Liebhafsky, H. A.; McGavock, W. C.; Reyes, R. J.; Roe, G. M.; Wu, S. L. *J. Am. Chem. Soc.* **1978**, *100*, 87. (e) Liebhafsky, H. A.; Furruichi, R.; Roe, G. M. *J. Am. Chem. Soc.* **1981**, *103*, 51.

(3) Peard, M. G.; Cullis, C. F. *Trans. Faraday Soc.* **1951**, *47*, 616. (b) Degn, H. *Acta Chem. Scand.* **1967**, *21* (4), 26. (c) Sharma, K. R.; Noyes, R. M. *J. Am. Chem. Soc.* **1975**, *97*, 202. (d) Sharma K. R.; Noyes, R. M. *J. Am. Chem. Soc.* **1976**, *98*, 4345. (e) Noyes, R. M.; Field, R. J. *Acc. Chem. Res.* **1977**, *10*, 273. (f) Odutola, J. A.; Bohlander, C. A.; Noyes, R. M. *J. Phys. Chem.* **1982**, *86*, 818. (g) Anić, S.; Kolar-Anić, Lj. *Ber. Bunsen-Ges. Phys. Chem.* **1986**, *90*, 539. (h) Anić, S.; Kolar-Anić, Lj. *J. Chem. Soc., Faraday Trans.* **1988**, *84*, 3413. (i) Anić, S.; Stanisavljev, D.; Krnajski Belovljev, G.; Kolar-Anić, Lj. *Ber. Bunsen-Ges. Phys. Chem.* **1989**, *93*, 488. (j) Anić, S.; Kolar-Anić, Lj.; Stanisavljev, D.; Begović, N.; Mitić, D. *React. Kinet. Catal. Lett.* **1991**, *43*, 155. (k) Schmitz, G. In *Spatial Inhomogenities and Transient Behavior in Chemical Kinetics*; Gray, P., Nicolis, G., Borckmans, P., Scott, S. K., Eds.; Manchester University Press: Manchester, U.K., 1990; p 666. (l) Treindl, L.; Noyes, R. M. *J. Phys. Chem.* **1993**, *97*, 11354. (m) Stanisavljev, D.; Vukojević, V. *J. Serb. Chem. Soc.* **1995**, *60*, 1125. (n) Anić, S.; Kolar-Anić, Lj.; Kõrös, E. *React. Kinet. Catal. Lett.* **1996**, *57*, 37. (o) Stanisavljev, D. *Ber. Bunsen-Ges. Phys. Chem.* **1997**, *101*, 1036. (p) Anić, S.; Stanisavljev, D.; Cupić, Z.; Radenković, M.; Vukojević, V.; Kolar-Anić, Lj. *Science of Sintering* **1998**, *30*, 49. (q) Stanisavljev, D.; Begović, N.; Zujović, Z.; Vucelić, D.; Bacić, G. *J. Phys. Chem.* **1998**, *102*, 6883. (r) Stanisavljev, D.; Begović, N.; Vukojević, V. *J. Phys. Chem.* **1998**, *102*, 6887 and references therein.

(4) Chopin-Dumas, J. *C. R. Acad. Sci. Ser. C* **1987**, *287*, 553. (b) Chopin-Dumas, J.; Papel, M. N. In *Synergetics: Non-Equilibrium Dynamics in Chemical Systems*; Vidal, C., Pacault, A., Eds.; Springer-Verlag: New York, 1978; p 69. (c) Buchholtz, F. G.; Broecker, S. *J. Phys. Chem.* **1998**, *102*, 1556.

(5) Edelson, D.; Noyes, R. M. *J. Phys. Chem.* **1979**, *83*, 212. (b) Schmitz, G. *J. Chim. Phys.* **1987**, *84*, 957. (c) Noyes, R. M. *J. Phys. Chem.* **1990**, *94*, 4404. (d) Kolar-Anić, Lj.; Schmitz, G. *J. Chem. Soc., Faraday Trans.* **1992**, *88*, 2343. (e) Noyes, R. M.; Kalachev, L. V.; Field, R. J. *J. Phys. Chem.* **1995**, *99*, 3514. (f) Kolar-Anić, Lj.; Miljenović, Dj.; Anić, S.; Nicolis, G. *React. Kinet. Catal. Lett.* **1995**, *54*, 35. (g) Kolar-Anić, Lj.; Cupić, Z.; Anić, S.; Schmitz, G. *J. Chem. Soc., Faraday Trans.* **1997**, *93*, 2147. (h) Kolar-Anić, Lj.; Cupić, Z.; Anić, S. *Hem. Ind.* **1998**, *52*, 337. (i) Cupić, Z.; Kolar-Anić, Lj. *J. Chem. Phys.* **1999**, *110*, 3951. (j) Cupić, Z.; Kolar-Anić, Lj. In *Advanced Sciences and Technology of Scintring*; Stojanović, B. D., Skoroklod, V. V., Nikolić, M. V., Eds.; Kluwer Academic/Plenum Publishers: New York, 1999; p 75 and references therein.

(6) Briggs, T. C.; Rauscher, W. C. *J. Chem. Educ.* **1973**, *50*, 496. (b) Furrow, S. D.; Noyes, R. M. *J. Am. Chem. Soc.* **1982**, *104*, 38. (c) Furrow, S. D.; Noyes, R. M. *J. Am. Chem. Soc.* **1982**, *104*, 42. (d) Noyes, R. M.; Furrow, S. D. *J. Am. Chem. Soc.* **1982**, *104*, 45. (e) De Kepper, P.; Epstein, I. R. *J. Am. Chem. Soc.* **1982**, *104*, 49. (f) Furrow, S. D. *Oscillations and Traveling Waves in Chemical Systems*; Mir: Moscow, 1988; Chapter 5. (g) Vukojević, V.; Graae Sørensen, P.; Hynne, F. *J. Phys. Chem.* **1993**, *97*, 4091. (h) Vukojević, V.; Graae Sørensen, P.; Hynne, F. *J. Phys. Chem.* **1996**, *100*, 17175.

(7) Vukojević, V.; Pejić, N.; Stanisavljev, D.; Anić, S.; Kolar-Anić, Lj. *Analyst* **1999**, *124*, 147.

(8) Terlecki-Baricević, A.; Cupić, Z.; Anić, S.; Kolar-Anić, Lj.; Mitrovski, S.; Ivanović, S. *J. Serb. Chem. Soc.* **1995**, *60*, 969.

(9) Anić, S.; Kolar-Anić, Lj. *Ber. Bunsen-Ges. Phys. Chem.* **1986**, *90*, 1084.

(10) Hassard, B. D.; Kazarinoff, N. C.; Wan, Y.-H. *Theory and Application of Hopf Bifurcation*; University Press: Cambridge, U.K., 1981.

(11) Maselko, J. *Chem. Phys.* **1982**, *67*, 17. (b) Mankin, J. C.; Hudson, J. L.; *Chem. Eng. Sci.* **1984**, *39*, 1807. (c) Noszticzius, Z.; Wittman, M.; Stirling, P. *J. Chem. Phys*, **1987**, *86*, 1922. (d) Gáspár, V.; Peng, B.; Showalter, K. In *Spatial Inhomogenities and Transient Behavior in Chemical Kinetics*; Gray, P., Nicolis, G., Borckmans, P., Scott, S. K., Eds.; Manchester University Press: Manchester, U.K., 1990; p 279. (e) Olsen, R. J.; Epstein,

I. R. *J. Chem. Phys.* **1991**, *94*, 3083. (f) Scott, S. K. *Chemical Chaos*; Clarendon Press: Oxford, U.K., 1991. (g) Stemwedel, J. D.; Ross, J.; Schreiber, I. *Adv. Chem. Phys.* **1995**, *89*, 327.

(12) Nicolis, G. *Self-organization in Nonequilibrium Systems*; Wiley: New York, 1977. (b) Drazin, P. G. *Nonlinear Systems*; University Press: Cambridge, U.K., 1994. (c) Nicolis, G. *Introduction to Nonlinear Science*; University Press: Cambridge, U.K., 1995. (d) Acheson, D. *From Calculus to Chaos*; Oxford University Press: Oxford, U.K., 1998.

(13) Noszticzius, Z.; Stirling, P.; Wittmann, M. *J. Phys. Chem.* **1985**, *89*, 4914.

(14) Anić, S.; Cupić, Z.;]irić, J. In *Physical Chemistry '94*; Ribnikar, S., Ed.; DFHS: Belgrade, 1994; p 141.